$^{40}Ca(n, \alpha)^{37}Ar$ Reaction at 14.1 MeV

CHUNG-CHAUR PERNG (彭忠朝), SONG-YUNG LIN (林松雲),
MUH-CHUEN CHOU (周木春), YI-CHUAN Hsu (許玉釧),
JENN-LIN HWANG (黃振麟) and YUIN-CHI Hsu (許雲基)

Department of Physics, National Taiwan University
Taipei, Taiwan

(Received 8 August 1973)

Alpha particles produced by the interaction of 14.1 MeV neutrons with ^{40}Ca have been studied by using counter telescope technique.

The well resolved groups of the alpha particles leading to $^{37}Ar^{*}=0$, 1.41-1.61 and 2.22-3.52 MeV states were obtained. The strong forward peak in the angular distributions of these groups suggests a large contribution from direct reaction process, in contrast with the earlier investigations. The angular distribution of the ground state was analyzed with the incoherent combination of direct reaction process using DWBA method, and compound nucleus process by Hauser-Feshbach theory. The cross section of the ground state transition was found to be 1.7f0.2 mb, in which the contribution due to compound nucleus process was less than 12%.

For the unresolved groups of the alpha particles, corresponding to the highly excited states of ^{37}Ar the angular distribution is approximately symmetrical with respect to 90°, and is agreeable with the prediction of compound nucleus process. From the analysis of these groups, the level density parameter, nuclear temperature and spin cut-off parameter are evaluated.

1. INTRODUCTION

THE (*n*, a) reaction induced by 14.1 MeV neutrons for medium weight nuclei has been investigated for many elements.[1-4] Most of these reactions have been found to proceed principally through compound nucleus process. However, several recent results[2-4] on the angular distributions leading to low-lying states, have shown obvious peak in the forward direction as expected fi-om the, direct interaction process. In view of the scarce and inconsistent experimental results, we decide to measure the energy and angular distributions of the alpha particles from the $^{40}Ca(n,\alpha)^{37}Ar$ reaction.

(1) 0. N. Kaul, Nuclear Physics 55, 127 (1964); U.Seebeck and M. Bormann, Nuclear Physics 68, 387 (1965); Y. C. Hsu et *al.*, Chinese J. Phys. 3, 90 (1965).
(2) I. M. Turkiewicz, N. Cindro, P. Kulišič, P. Strobal and D. Veselič, Nuclear Physics 77, 276 (1966).
(3) C. Spira and J. M. Robson, Nuclear Physics **A127**, 81 (1969); S. Kardonsky, H.L. Finston and E.T. Williams, Phys. Rev. C4, 840 (1971).
(4) M. Bormann, W. Schmidt, V. Schröder, W. Scobel and U.Seebeck, Nuclear Physics A186, 65 (1972).

2. EXPERIMENTAL PROCEDURE

The calcium target of natural isotopic constitution used in this work was of 2.0 cm diameter and 2.04 mg/cm^2 thickness evaporated on a 2.0 mg/cm^2 thick gold foil. For the measurement of the background a gold foil of the same stopping power was used. The abundance of ^{40}Ca in natural calcium is 97%. However, ^{40}Ca has the highest Q-value for (n, α) reaction of all natural isotopes of calcium, thus, the contribution from the other isotopes present in the Ca target could be neglected.

A 150 keV beam of deuterons was used to produce an average flux of 2×10^9 neutrons/sec (into 4π) via the $T(d, n)\,^4He$ reaction. The neutrons were monitored by counting the associated alpha particles from the $T(d, n)\,^4He$ reaction with a CsI(Tl) scintillation counter.

The alpha particles emitted from the calcium target were detected by a $\Delta E-E$ counter telescope[5] shown in Fig. 1. The counter telescope consists of three proportional counters (A, B and C) and a surface barrier detector (D) just thick enough to stop the most energetic alpha particles. To reduce the background, the walls of the telescope are lined with 0.1 mm thick tantalum. The counters are filled to a pressure of 10 cmHg with a mixture of 95% Ar and 5% CH_4. The anode wires are of 0.1 mm diam. tungsten and are covered at the ends with gold sleeves to limit the sensitive volume.

The counter (A) is placed in front of the Ca target. Its role is to reject the tripple coincidence due to charged particles from the silicon detector proceeding backward through B and C counters and due to particles from the front wall of the telescope chamber. This counter is in anti-coincidence with the other three counters. The counter B reduces the background and helps to collimate the emitted particles. The counter C is used to determine the energy loss ΔE of a particle which passed through it. The surface barrier detector D measures the residual energy of the same particle. The telescope and the target-holder are placed in a cylindrical stainless steel chamber. The chamber is set on a turn-table in whose axis the target-holder is mounted and is placed with the target-holder at 10 cm distance from the neutron source in a direction at 90° to the deuteron beam.

The construction of the target-holder allows to choose any sample among three targets and a ^{241}Am–α source without destroying the vacuum. The mean value of angles θ between the direction of the incident neutron on the Ca target and that of emitted alpha particle, was calculated with Newton-Cotes method.[6]

(5) M. Brendle, M. Mõrike, G. Staudt and G. Steidle, Nucl. Instr. and Meth. **81**, 141 (1970); S. Shirato and N. Koori, Nucl. Instr. and Meth. 57, 325 (1967).
(6) C.C. Wung, M. S. Thesis, Taiwan University, (unpublished 1971).

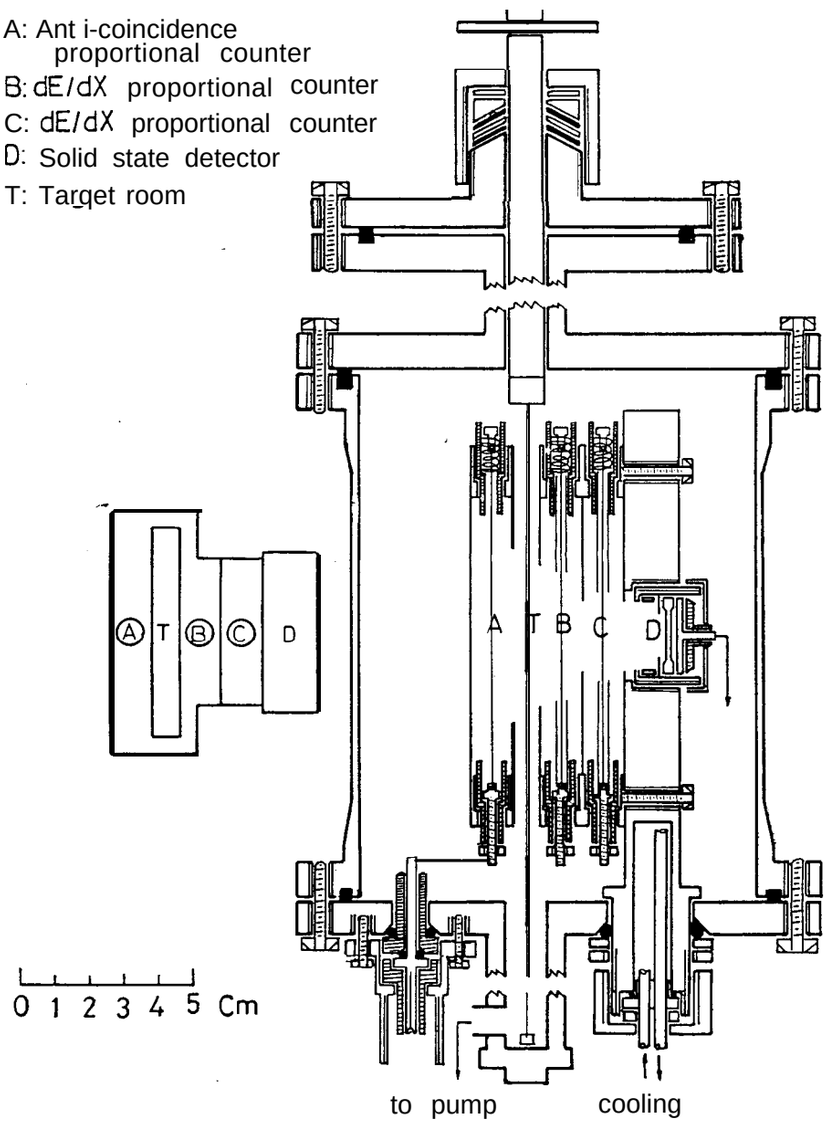

Fig. 1. Construction of counter telescope.

In Fig. 2 is shown a block diagram of the electronics, in which a ***AE-E*** particle identification system using an X-Y oscilloscope is employed. The tripple coincidence pulse intensifies the oscilloscope cathode-ray beam (Z-axis) when the X(E) and the $Y(\Delta E)$ pulse are at their maximum, resulting in generation of a bright spot on the oscilloscope screen. After long time run, the spots thus generated would form hyperbolic traces depending on the type and energy of the particle. By masking other parts than a-hyperbola and viewing it with a photo-multiplier, a gate pulse is generated and used to open a pulse height analyzer.

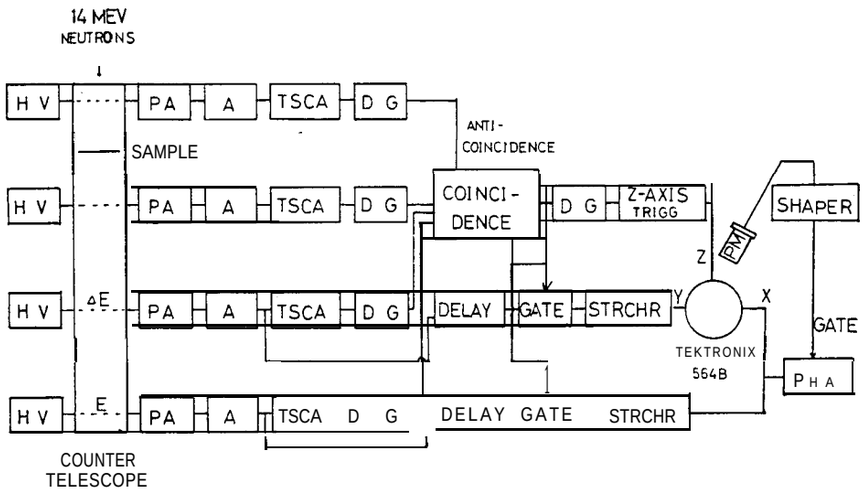

Fig. 2. Schematic diagram of the counter telescope.
TSCA-timing single channel analyzer; PA-preamplifier; A-amplifier; DG-delay generator.

The energy resolution of the system at alpha particle energy 12 MeV is about 450 keV, which may be mainly attributed to the target thickness. The background in the telescope at alpha particle energy below 6 MeV was considerably higher and made higher excited state transitions difficult to measure. This background was mainly due to low energy particles traveling backwards from the surface barrier detector.

3. METHODS OF ANALYSIS

3-1. DWBA analysis

The *DI* contribution including knock-on and pick-up modes were performed by using the computer code INS-DWBA-3.[7] The calculation was programed for NTU CDC-3150 computer and was divided into several overlay links using disk storage for arrays. The form of potential used is

$$U(r) = U_c(r) - Vf(r) - iWg(r) + V_{s.o.}(r), \qquad (1)$$

where $U_c(r)$ is the Coulomb potential of a uniformly charged sphere of radius $r_0 = r_c A^{1/3}$ and f(r), a Woods-Saxon form factor is

$$f(r) = \left[1 + \exp\left(\frac{r - r_R A^{1/3}}{a_R}\right)\right]^{-1} \qquad \text{for all particles.} \qquad (2)$$

The absorption potential form factors with surface or a volume form used are

(7) T. Une, T. Yamazaki, S. Yamaji and Yoshida, INS-PT-10 (1965).

$$g_{surf}(r) = exp\left[-\left(\frac{r - r_I A^{1/3}}{a_I}\right)^2\right] \qquad \text{for nucleons,} \qquad (3)$$

$$g_{vol}(r) = \left[1 + \exp\left(\frac{r - r_I A^{1/3}}{a_I}\right)\right] \qquad \text{for a -particle.} \qquad (4)$$

The spin-orbit potential is of the form

$$V_{s.o.}(r) = 2\left(\frac{\hbar}{m_\pi c}\right)^2 V_{s.o.} \frac{\mathbf{l}\cdot\mathbf{s}}{r} \frac{d}{dr}\left\{\left[1 + \exp\left(\frac{r - r_R A^{1/3}}{a_R}\right)\right]\right\}. \qquad (5)$$

Since detailed alpha and neutron elastic-scattering data at the relevant energies are not available for the present reaction, the alpha particle potential is obtained by averaging the parameters obtained by Gaul et *al.*[8] and Wallace et *al.*[9] for the scattering of alpha particles. on ^{36}Ar at 15-25 MeV, and for the neutron potential, the parameters are deduced from the results of Hodgson.[10] A single set of optical parameters is used and listed in Table I.

Table I. Optical-model parameters used in DWBA analysis

Channel	V (MeV)	r_R (fm)	a_R (fm)	W (MeV)	r_I (fm)	a_I (fm)	$V_{s.o.}$ (MeV)	r_c (fm)
$n + {}^{40}Ca$	43.8	1.25	0.65	11.3	1.25	0.98	0.0	1.25
$a + {}^{37}Ar$	180.5	1.70	0.59	26.6	1.70	0.30	0.0	1.70

In the DWBA calculation, the harmonic oscillator bound state wave are assumed. The number of nodes (N) in the radial parts and orbital angular momentum quantum number (l) for the initial and final bound states are shown in Table II. The harmonic oscillator parameter is determined by the common rule $\nu = 0.96\, A^{-1/3}\, fm^{-2}$.[11]

Table II. Bound state quantum number for the $^{40}Ca(n, \alpha_0)^{37}Ar$ reaction

Knock-on	$^{40}Ca : (^{36}Ar + {}^4He)$	Es
	$^{37}Ar : (^{36}Ar + n)$	$1d$
Pick-up	$^{40}Ca : (^{37}Ar + {}^3He)$	$3d$
	$^4He : (^3He + n)$	$1s$

(8) G. Gaul, H. Lüdecke, R. Santo, H. Schmeing and R. Stock, Nuclear Physics **A137**, 177 (1969).
(9) W. J. Wallace, K. R. Knuth and R. H. Davis, Phys. Rev. **C2**, 1738 (1970).
(10) P. E. Hodgson. ***Direct Interactions*** and ***Nuclear Reaction Mechanism*** (Gordon and Breach, Science Publishers, Inc. New York, 1963) P. 103.
(11) B.H. Wildenthal, E.C. Halbert, J.B. McGrory and T.T. S. Kuo, Phys. Rev. C4, 1266 (1971).

3-2. Compound nucleus analysis

The compound nucleus calculation was based on the Hauser-Feshbach formalism as described in ref.[12] The differential cross section was given by

$$\frac{d\sigma}{d\Omega}(\theta) = \frac{1}{4k^2(2i+1)(2I+1)} \sum_{slJL} (-)^{s'-s} \cdot \frac{T_l(\alpha) \cdot T_{l'}(\alpha')}{G(J)} \times Z(lJlJ; sL) \cdot Z(l'Jl'J; s'L) \cdot P_L(\cos\theta) , \quad (6)$$

where J is the spin of the compound nucleus, I and i are the spins of the target and the projectile nucleus respectively, α and a ' label the incoming and outgoing pair of particles and their states of excitation, s is the channel spin and k is the wave number for the incident particle. The quantities $T_l(\alpha)$ are the quantum mechanical penetrabilities for incoming and outgoing particles of angular momentum l. The Z is the coupling coefficient defined in ref.[13] and $P_L(\cos\theta)$ is Legendre polynomial of order L. The primed quantities listed above denote the exit channel and the summation includes only terms of like parity.

A difficulty in evaluating Eq. (6) is the occurence of the term G(J), because it involves all open exit channels in which the compound nucleus can decay. This term can be calculated, however, according to the method of Towle[14] and Renclic,[15]

$$G(J) = \sum_b \left(\sum_{sl} T_l(\varepsilon) + \sum_{sl} S(J, l) \cdot \int T_l(\varepsilon)\, W(E)\, dE \right). \quad (7)$$

In Eq. (7), b refers to all possible outgoing particles with energy ε and s, l defined as in Eq. (6). The first term describes the discrete levels of known excitation energy E, spin and parity. The integration in the second term includes the levels of the continuous region and the unknown excitation energy or quantum numbers. The spin distribution function $S(J, l)$ is of the form[15]

$$S(J, l) = \exp\left(-\frac{(J-l)^2}{2\sigma^2}\right) - \exp\left(-\frac{(J+l+1)^2}{2\sigma^2}\right). \quad (8)$$

Using a Fermi-gas formula modified for pairing effects, the density of levels of all spins is given by[16]

$$W(E) = [ta^{1/2}/12 \cdot 2^{1/2}(I/\hbar^2)^{1/2} \cdot (E + t - P)^{2}] \cdot \exp[2a^{1/2}(E-P)^{1/2}], \quad (9)$$

(12) W. Hauser and H. Feshbach, Phys. Rev. 87, 366 (1952); H. Feshbach, *Nuclear Spectroscopy*, part B, ed. by F. Ajzenberg-Selove (Academic Press, New York, 1960) P. 661.
(13) J. M. Blatt and L.C. Biedenharn, Rev. Mod. Phys. 24, 258 (1952).
(14) J. H. Towle and R. 0. Owens, Nuclear Physics **A100**, 257 (1967).
(15) D. Rendič, B. Antolkovič, G. Paič, M. Turk and P. Tomas, Nuclear Physics All?, 113 (1968).
(16) A. A. Katsanos, R. W. Shaw, Jr., and R. Vandenbosh, Phys. Rev. Cl, 594 (1976).

where a is the level density parameter, P is the pairing energy correction,[17] t is the thermodynamic temperature given by

$$E - P = at^2 - t, \tag{10}$$

and **Z** is the nuclear moment of inertia. The spin cut-off parameter σ in Eq. (8) can be related to the moment of inertia and the temperature t by

$$\sigma^2 = \mathcal{I} t/\hbar^2 . \tag{11}$$

The Fermi-gas model predicts that the moment of inertia is that of a rigid body, which for an infinite square well[18] is

$$\mathcal{I}_r = \frac{2}{5} MR^2 , \tag{12}$$

where M is the mass of the nucleus and $R = 1.2 \times A^{1/3}$ is the nuclear radius.

The transmission coefficient was extracted from a modified version of the computer code INS-DWBA-1.[19] The optical potential is of the same form as Eq. (1) and the parameters are listed in Table III. All energetically possible n, p and a exit channels were considered. The lth particle with projectile spin j are given by $T_{l,j}$ and the average transmission coefficient[20] is defined for neutrons and protons by

$$T_l = \frac{l+1}{2l+1} T_{(l, j=l+1/2)} + \frac{l}{2l+1} T_{(l, j=l-1/2)} . \tag{13}$$

For a-particles, it follows that $T_l = T_{l,j}$.

Table III. Optical-model parameters used in compound nucleus calculation

Channel	V (MeV)	r_R (fm)	a_R (fm)	W (MeV)	r_I (fm)	a_I (fm)	$V_{s.o.}$ (MeV)	r_c (fm)
$n + {}^{40}$Ca	$48.0 - 0.3E$	1.25	0.65	$3.0E^{1/2}$	1.25	0.95	$22.0 - 0.3E$	1.25
$p + {}^{40}$K	$58.0 - 0.3E$	1.25	0.65	$3.0E^{1/2}$	1.25	0.95	$22.0 - 0.3E$	1.25
α + ^{37}Ar	180.5	1.70	0.59	26.6	1.70	0.30	0.0	1.70

4. RESULTS AND DISCUSSION

An example of the energy spectrum of the emitted a-particles measured at $\bar{\theta} = 14.9°$ is shown in Fig. 3, where the background has been subtracted. Three sharp peaks are observed. The first peak corresponding to the ground state is

(17) A. G. W. Cameron, Can. J. Phys. 36, 1040 (19%).
(18) C. Bloch, Phys. Rev. 93, 1094 (1954).
(19) M. Kawai et al., INS-PT-8 (1965).
(20) D. G. Swanson and N. T. Porile, Phys. Rev. **Cl,** 14 (1970).

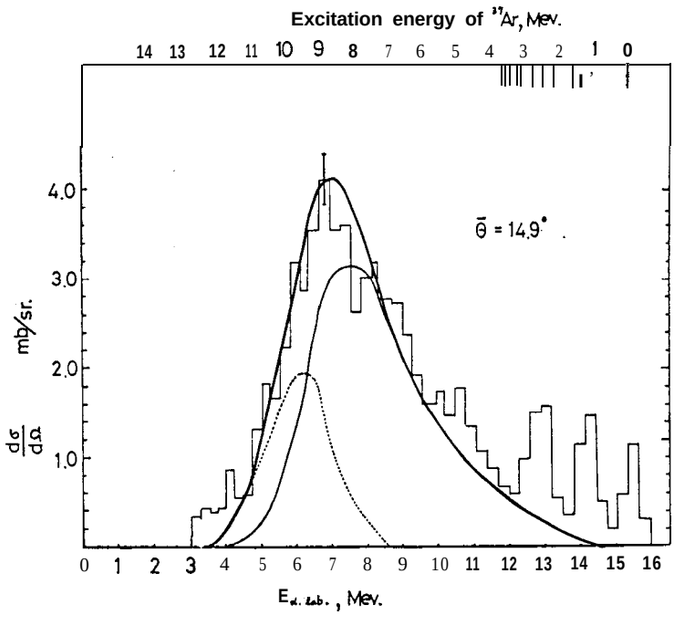

Fig. 3. Energy spectrum of the alpha particles emitted from the $^{40}Ca(n,\alpha)^{37}Ar$ reaction. Solid and dotted curves represent the contributions from the (n, a) and $(n,n'\alpha)$ spectra predicted by the statistical theory, assuming the constant nuclear temperature formula for the level density with $T=1.32$ and $T=0.55$ MeV respectively.

separated with fair resolution. The second peak corresponds to the 1.41+1.61 MeV states which are too close to be resolved. The same feature is found in the third peak. The angular distributions of a-particles leading to various excitation energies of ^{37}Ar are shown in Fig. 4. The angular distributions of the first three a-particle groups (Fig. 4a–c) show a predominant forward peak which might be due to direct process, but such a peak is not found appreciably in the earlier work.[2]

For the highly excited states of ^{37}Ar, the angular distributions shown in Fig. 4d–e are nearly symmetric with 90°, indicating the process of compound nucleus mechanism.

Because of the 14.1 MeV bombaring energy and medium weight target nucleus used in this study it is not possible to dismiss the effects of compound-nucleus formation(“). Therefore, the theoretical calculations were given by the incoherent sum of the direct contribution and the compound nucleus term

$$\frac{d\sigma}{d\Omega_{exp}} = D\frac{d\sigma}{d\Omega_{DI}} + C\frac{d\sigma}{d\Omega_{CN}}. \qquad (14)$$

(21) N. Cindro. Revs. Mod. Phys. 38, 391 (1966).

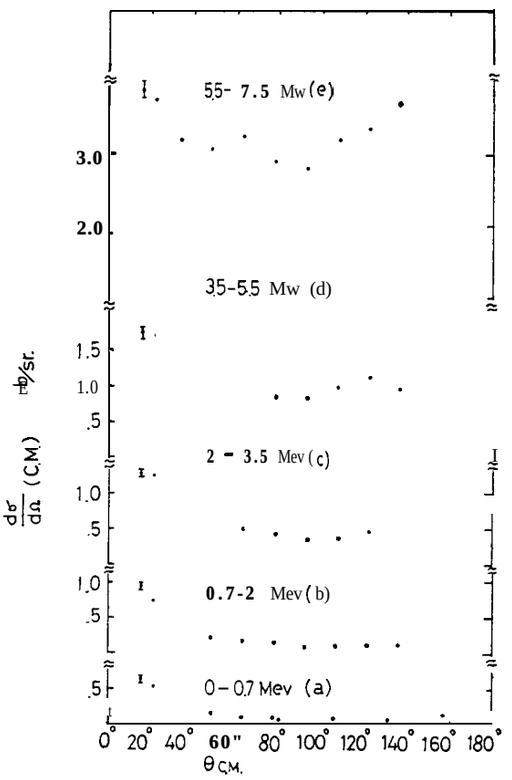

Fig. 4. Angular distributions of alpha particles leading to various excitation energies of ^{37}Ar.

The factor C weighting the compound nucleus contribution is restricted to positive value between 0 and 1.[22] This is needed since the Hauser-Feshbach theory does not presently make an adequate provision for the loss of flux due to direct reaction processes.

The incoherent sums of pick-up+ CN and knock-on+CN are done for the ground-state transition, as shown in Fig. 5. Both are in good agreement with the experimental results. The compound nucleus contributions plotted have been reduced by the C-coefficient of 0.1, which was found by least squares method. The cross section of the ground state transition is obtained to be 1.7 ± 0.2 mb. In the case of doublet (1.41+ 1.61 MeV states), it contains too many possible mechanisms, the superposition as stated above is beyond the scope of the present paper and thus only the experimental results are shown. The angular distribution belonging to 2.22-3.52 MeV excitation states also has strong resemblance to the above shapes.

(22) P. D. Georgopulos, W. A Lochstet and E. Bleuler, Nuclear Physics **A183**, 625 (1972).

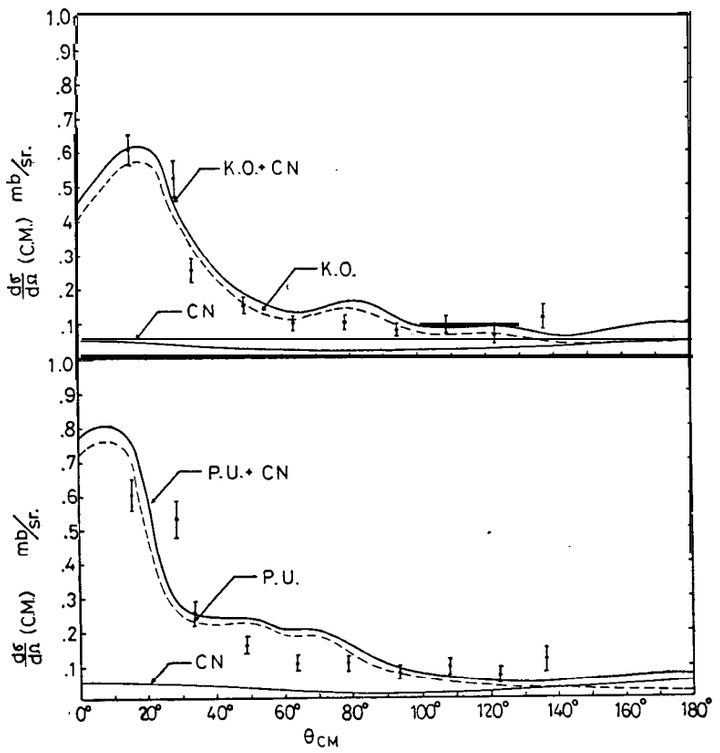

Fig. 5. Angular distribution of the ground state transition with curve from an incoherent sum of *DI* and CN calculations, for $c=0.1$.

Since the compound nucleus mechanism is not playing the predominant role in these resolved groups, the variations of the level density parameter a and spin cut-off parameter σ are not sensitive enough to affect the shape of the compound nucleus cross section. However, in order to extract the parameters and nuclear temperature T, we used the following two approximations of the level density in Es. (9) of the residual nucleus at excitation energy E: $W(E) \propto \exp(E/T)$ and W(E) $\propto E^{-2} \exp 2(aE)^{1/2}$. The function W(E) is related to the number N(E) of alpha particles emitted at energy ε by the statistical model as

$$N(E) \,.\, d\varepsilon \propto \sigma_c(\varepsilon) \,.\, W(E) \,.\, d\varepsilon, \tag{15}$$

where $\sigma_c(\varepsilon)$ is the inverse cross section for the formation of a compound nucleus by alpha particles of energy ε, and can be calculated in term of $T_l(\varepsilon)$ according to the method stated in Sec. 3. The functions $\ln N(\varepsilon)/\varepsilon\sigma_c(\varepsilon)$ and ln N(E) $E^2/\varepsilon\sigma_c(\varepsilon)$ show a linear dependence on E and $E^{1/2}$, respectively. Except for low alpha energy, most of the experimental points show a linear dependence as given in Fig. 6. Due to the Q-value ($Q(n,\alpha)=1.75$ MeV, $Q(n,n'\alpha)$ =-7.04 MeV) and the Coulomb barrier effect, the systematic deviation from the line at small alpha

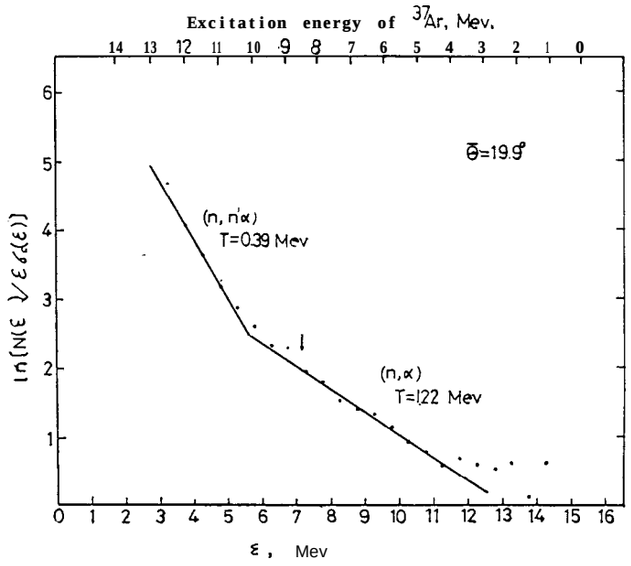

Fig. 6. Constant-temperature plots for alpha particle spectra. Arrow corresponds to the maximum energies of alpha particles from the (n, $n'\alpha$) reactions.

energies is consisdered to be attributed to the reaction $^{40}Ca(n,n'\alpha)^{36}Ar$. From the slope of the logarithmic plots, the parameter T = 1.27 ± 0.11 MeV and a=7.03 ± 0.60 MeV^{-1} for ^{37}Ar and T=0.47 ± 0.15 MeV for ^{36}Ar are obtained. The combination of (n, n ' a) and (n, a) spectrum predicted by the statistical theory on the basis of the Maxwellian alpha energy distribution are also shown in Fig. 3. To estimate the magnitude of the spin cut-off parameter σ, we fitted the angular distribution for the energy region of $^{37}Ar^*$ =3.5–5.5 MeV (Fig. 4b), where the contribution from (n, n ' a) and direct interaction might be neglected, by the formula[23] $W(\theta)$ = const . $1+1/12\,(J^2 \cdot l^2/\sigma^4)\,P_2(\cos\theta)$, J and l being the mean square of the compound nucleus spin and the angular momentum of the emitted particles, respectively. The parameter σ is found to be 2.68±0.50 for the residual nucleus ^{37}Ar.

ACKNOWLEDGMENTS

The authors would like to express their appreciation to Dr. C. L. Lin for supplying DWBA computer programs for data analysis.

This work was supported by the National Council on Science Development.

(23) W. J. Knox, A. R. Quinton and C. E. Anderson, Phys. Rev. **120**, 2120 (1960).